# Photoreductive Chlorine Elimination from a Ni(III)$Cl_2$ Complex Supported by a Tetradentate Pyridinophane Ligand

*Hanah Na,[a] Michael B. Watson,[b] Fengzhi Tang,[b] Nigam P. Rath,[c] and Liviu M. Mirica[a]**

[a]*Department of Chemistry, University of Illinois at Urbana-Champaign, Urbana, Illinois, 61801*
[b]*Department of Chemistry, Washington University, St. Louis, Missouri, 63130-4899*
[c]*Department of Chemistry and Biochemistry, University of Missouri – St. Louis, St. Louis, Missouri, 63121-4400*

**E-mail: mirica@illinois.edu*

**Abstract:**

Herein we report the isolation, characterization, and photoreactivity of a stable $Ni^{III}$ dichloride complex supported by a tetradentate pyridinophane N-donor ligand. Upon irradiation, this complex undergoes an efficient photoreductive chlorine elimination reaction, both in solution and the solid-state. Subsequently, the $Ni^{III}Cl_2$ species can be regenerated via a reaction with $PhICl_2$.

## Introduction

Photoreductive halogen elimination reactions are of growing interest due to their relevance to the photodriven HX-splitting reactions, which have been considered promising chemical strategies for solar-to-fuel energy conversion.[1-4] Most commonly, precious 2nd and 3rd row transition metal complexes of Ir, Au, or Rh are exploited for this type of reaction due to their favorable photophysical and photochemical properties.[5-13] However, for a

sustainable system, it is imperative to replace precious metal ions with earth-abundant 1st row metal ions.[14,15] Recent work from Nocera *et al.* demonstrated efficient halogen elimination photoreactions from $Ni^{III}$ trihalide complexes supported by bidentate phosphine ligands.[16,17] The targeted design strategy is inspired by the seminal work of Hillhouse, where reductive elimination from a $Ni^{III}$ state is preferred over a $Ni^{II}$ state.[18-21] Instead of accessing a $Ni^{III}$-like state via excitation of $Ni^{II}$ species into the metal-to-ligand charge transfer (MLCT) state, starting with a $Ni^{III}$ complex would circumvent the inherent drawback of short excited-state lifetimes for the 1st row transition metal complexes.[22] More recently, Castellano *et al*. showed visible light-induced Cu–Cl homolytic bond cleavage reaction in $[Cu(dmp)_2Cl]^+$.[23] Nevertheless, beyond the above examples little progress has been made toward a photoreductive halide elimination reaction from other 1st row transition metal complexes, and therefore more diverse molecular platforms that support such a reaction need to be identified. We note that photoelimination reactivity examples of $Ni^{III}$ complexes supported by N-donor ligands are very rare, partially due to the instability of these complexes that prevents their detailed characterization. In recent years, photocatalytic generation of chlorine radicals from $(bpy)Ni^{III}$ complexes and their use in photoredox cross-coupling catalysis has been reported by Doyle *et al*. and Molander *et al*.[24-27] Despite the prevalence of chlorine photoelimination reaction from high-valent Ni species in these proposed mechanisms, little is known about their photophysics and photochemistry. This emphasizes the need to investigate the photoreactivity of isolated high-valent Ni complexes supported by N-donor ligands.

Our group has employed the tetradentate N-donor ligands *N,N*-dialkyl-2,11-diaza[3.3](2,6)pyridinophane ($^R$N4, R = Me, *i*Pr, *t*Bu) to stabilize various mononuclear

high-valent Ni complexes and investigate their C–C/C–heteroatom bond formation reactivity.[28-32] Accordingly, we postulated that this ligand system could be exploited to stabilize $Ni^{III}$ dihalide species, and therefore allow us to investigate their photoreactivity. Herein, we report the isolation, characterization, and photoreactivity study of a stable $Ni^{III}$ dichloride complex supported by the tetradentate pyridinophane ligand $^{Me}$N4, $[^{Me}N4Ni^{III}Cl_2]^+$ (**1**$^+$). Although several N-donor supported $Ni^{III}$ monochloride species,[33,34] porphyrin $Ni^{III}$ dibromide complexes,[35] and mixed N/C-donor supported $Ni^{III}$ halide complexes[30,36-43] were reported, none of them were studied in terms of their photochemistry. To the best of our knowledge, **1** represents the first isolated all N-donor supported $Ni^{III}$ chloride complex for which its photochemistry was investigated.

## Results and discussion

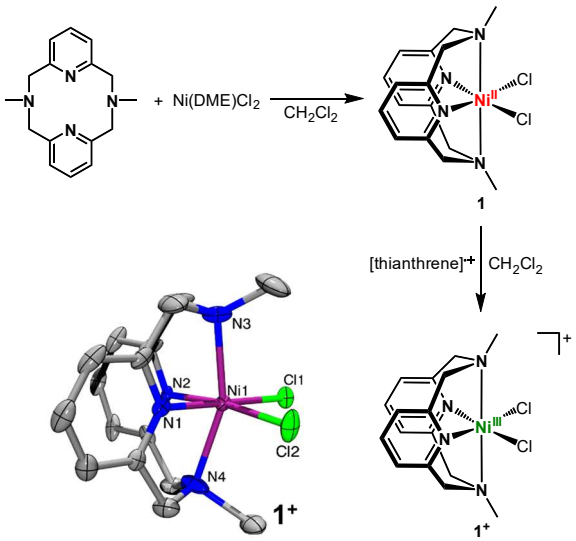


**Figure 1.** Synthesis of $^{Me}N4Ni^{II}Cl_2$ (**1**) and $[^{Me}N4Ni^{III}Cl_2]^+$ (**1**$^+$) complexes and ORTEP representation of the cation of [**1**]$PF_6$. Ellipsoids are shown at 50% probability level, with hydrogen atoms, counterion and an outer-sphere solvent molecule eliminated for clarity. Selected bond lengths (Å): Ni1–N1 1.900(3), Ni–N2 1.869(9), Ni–N3 2.159(3), Ni–N4 2.159(3), Ni–Cl1 2.2138(9), Ni–Cl2 2.1885(9).

The green complex $^{Me}$N4Ni$^{II}$Cl$_2$ (**1**) was prepared by stirring $^{Me}$N4 and Ni(DME)Cl$_2$ in $CH_2Cl_2$ overnight (Figure 1).[31] The cyclic voltammetry (CV) of **1** exhibits a pseudo-reversible oxidation wave at 0.52 V vs $Fc^{+/0}$, followed by an irreversible oxidation at 0.97 V vs $Fc^{+/0}$ (Figure S1). The first oxidation wave is assigned to the $Ni^{III}/Ni^{II}$ couple and this oxidation potential is similar to the reported value of $Ni^{III}/Ni^{II}$ couple for $^{tBu}$N4NiCl$_2$ of 0.52 V vs $Fc^{+/0}$, indicating a minimal effect of the axial N-substituents.[44] As the oxidation potential is chemically accessible, complex **1** can be easily oxidized with 1 equiv thianthrenyl tetrafluoroborate, resulting in [$^{Me}$N4Ni$^{III}$Cl$_2$]BF$_4$ ([**1**]BF$_4$) and as evidenced by an immediate color change from light green to dark purple. The effective magnetic moment $\mu_{eff}$ of 2.13 $\mu_b$, determined using the $^1$H NMR Evans method, is consistent with an S = 1/2 ground state for **1**$^+$, as expected for a $Ni^{III}$ center.[45,46] Interestingly, **1**$^+$ was stable at room temperature as a solid or in solution, showing minimal decomposition unless it was exposed to water (Figure S3), unlike other known N-donor supported $Ni^{III}$ mono or dichloride complexes that exhibit limited stability in solution at room temperature.[33,34,44] Single crystals of [**1**]PF$_6$ suitable for X-ray diffraction were grown via the diffusion of pentane into a $CH_2Cl_2$ solution of the complex. The complex [**1**]PF$_6$ shows the presence of a $Ni^{III}$ center that adopts a distorted octahedral geometry, with coordination to two pyridines and two amines of the $^{Me}$N4 ligand (Figure 1). The average axial Ni–$N_{ax}$ bond distance (2.159 Å) is substantially longer than the equatorial Ni–$N_{eq}$ bond distance (1.885 Å). The average Ni–Cl bond length (2.201 Å) is slightly shorter than those of other reported N-donor supported $Ni^{III}$ monochloride complexes (2.572 Å),[34] and similar to those of pincer-type $Ni^{III}$ chloride species (2.286 or 2.276 Å)[37,41] or the $Ni^{III}$ complexes supported by phosphine

ligands (2.219–2.287 Å).[16,17] The density functional theory (DFT) optimized geometry of $\mathbf{1}^+$ exhibits a slightly longer average bond lengths (Ni–$N_{eq}$ 1.9247 Å, Ni–$N_{ax}$ 2.2199 Å, Ni–Cl 2.2438 Å) but overall they are in good agreement with the experimental values. The EPR spectrum of $\mathbf{1}^+$ exhibits a pseudoaxial signal with $g_x$, $g_y$, and $g_z$ values of 2.149, 2.149, and 2.027, respectively (Figure 2a). Superhyperfine coupling to the two axial nitrogen atoms ($I$ = 1), primarily in the $g_z$ direction ($A_{2N}$ = 18.5 G) was observed, consistent with formation of $d^7$ $Ni^{III}$ species with a S = 1/2 ground state in which the unpaired electron occupies primarily the $d_{z^2}$ orbital of the Ni center.[47-50] Additionally, the DFT calculated spin density supports a metal-based radical description for $\mathbf{1}^+$, and the predominant $d_{z^2}$ character of the unpaired electron (Figure 2b). The UV-visible absorption spectra of **1** and $\mathbf{1}^+$ were obtained in MeCN (Figure 3, top). The absorption spectrum of $Ni^{II}$ complex **1** is dominated by a band at 371 nm (ε = 328 $M^{-1}cm^{-1}$) and a much weaker band at 600 nm (ε = 20 $M^{-1}cm^{-1}$). On the other hand, the $Ni^{III}$ complex $\mathbf{1}^+$ exhibits a more intense band at 354 nm (ε = 1,948 $M^{-1}cm^{-1}$) and a low-energy absorption band at 563 nm (ε = 211 $M^{-1}cm^{-1}$).

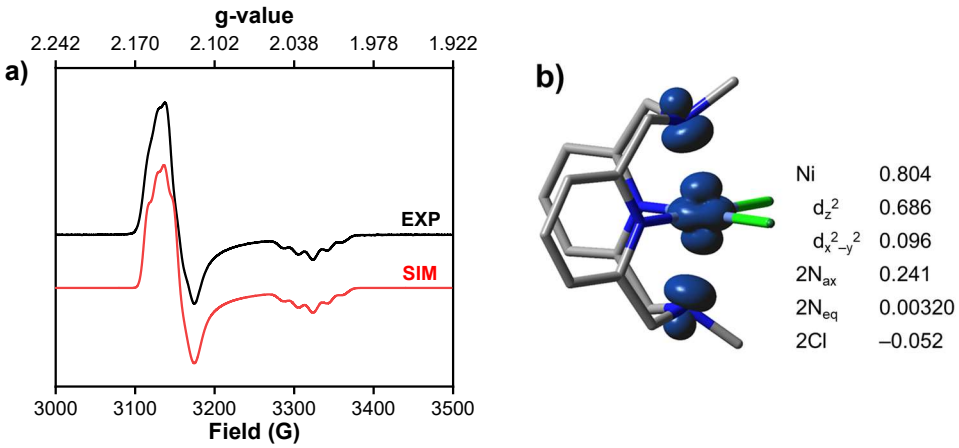


**Figure 2.** (a) Experimental (1:3 MeCN:PrCN, 77 K) and simulated EPR spectra of $\mathbf{1}^+$ using the following parameters: $g_x$ = 2.149, $g_y$ = 2.149, $g_z$ = 2.027, $A_x$(2N) = 12 G, $A_y$(2N) = 12 G, $A_z$(2N) = 18.5 G. (b) DFT calculated Mulliken spin density for $\mathbf{1}^+$ (shown as a 0.05 isodensity contour plot).

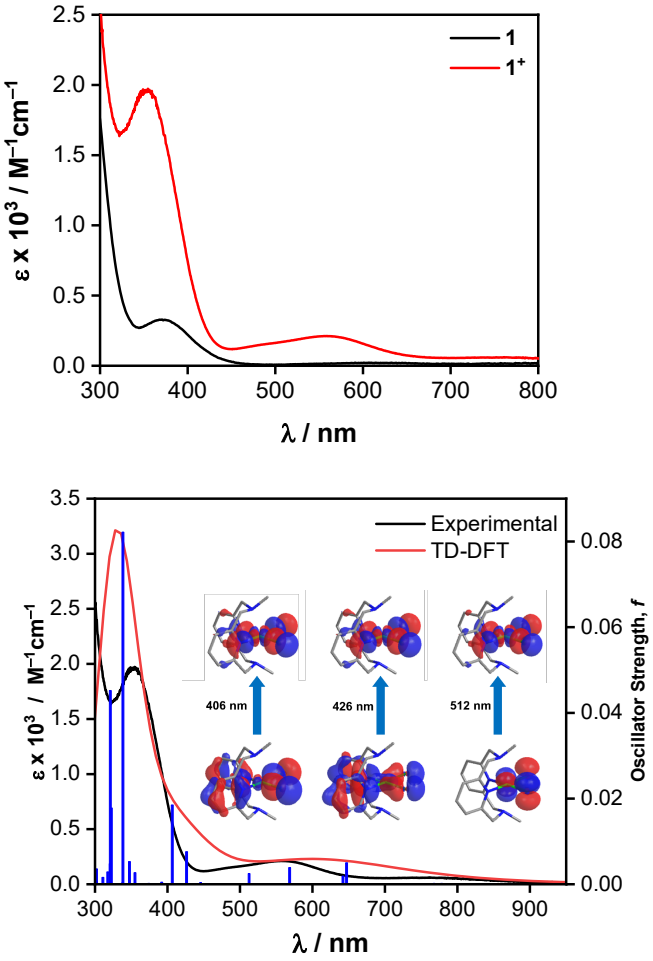


**Figure 3.** (Top) UV-vis absorption spectra of **1** (black solid line) and $\mathbf{1}^+$ (red solid line). (Bottom) Experimental (black solid line) and calculated (red solid line) UV-vis absorption spectra of $\mathbf{1}^+$ overlaid with oscillator (blue solid bars). Inset: The NTOs for the transitions associated with blue light (400–500 nm) excitation.

To probe the nature of the electronic transitions, time-dependent density functional theory (TD-DFT) calculations of $\mathbf{1}^+$ were performed using the B3LYP functional and the 6-31G* basis set. The simulated absorption spectrum matched closely with the experimental result (Figure 3, bottom). According to the calculations, the transitions in the blue region (400–500 nm) involve excited states that arise from the population of the

LUMOs possessing Ni–Cl σ* character (Figures S13–S15).[51] Natural transition orbitals (NTOs) analysis (Figure 3, bottom inset), which visualizes a localized picture of the transition density matrix,[52] confirms the assignment of the bands between 400 nm and 600 nm to ligand-to-metal charge transfer (LMCT) transitions, corresponding to the promotion of an electron from orbitals primarily localized on the $^{Me}$N4 ligand and/or the Cl ligand to the Ni–Cl antibonding MOs. The lower energy absorption bands at ~600 nm correspond to primarily d-d transitions (Figures S17 and S18). Overall, based on the TD-DFT calculations, excitation of $\mathbf{1}^+$ with blue LED irradiation would be expected to induce photoreduction of the complex with concurrent Ni–Cl bond dissociation.

In agreement with this spectroscopic assignment, irradiation of a MeCN solution of $\mathbf{1}^+$ with blue LED ($\lambda_{max}$ = 456 nm) resulted in a rapid quenching of the band at 563 nm, suggesting a facile photoreduction of the $Ni^{III}$ complex (Figure 5), while **1** did not display a significant spectral change over a longer time span (Figure S6). No olefinic traps were required to promote halogen elimination, and Cl-based products were not detected. This is reminiscent of the photoreactivity of the phosphine-$Ni^{III}$ trichloride complexes, where the photoeliminated chloride is trapped via H atom abstraction from the solvent.[16,17,33] The quantum yield ($\Phi_p$) of halogen elimination from $\mathbf{1}^+$ was determined to be 47% in MeCN, using potassium ferrioxalate as a chemical actinometer. The obtained quantum yield is comparable to the values for the phosphine-supported $Ni^{III}$ trichloride complexes, which range from 13% to 96%.[16,17]

The photoreduction reaction was also monitored by paramagnetic $^1$H NMR (Figure S7), and a comparison of the $^1$H NMR spectra with independently synthesized $Ni^{II}$ complexes identified the photoreduced product as the mono-solvento complex $[^{Me}N4Ni^{II}Cl(MeCN)]^+$

($\mathbf{2}^{+}$) instead of the bis-solvento complex $[^{Me}N4Ni^{II}(MeCN)_2]^{2+}$. The complex $\mathbf{2}^{+}$ can be synthesized independently through chloride abstraction with $KPF_6$ from **1** in MeCN. The structure of photoreduced product $\mathbf{2}^{+}$ was confirmed by single-crystal X-ray diffraction, albeit the MeOH analogue was characterized since diffraction-quality crystals could only be obtained in the presence of MeOH (Figure 4). Overall, an elongation of all Ni–X bond distances (X = N or Cl) compared to those of $\mathbf{1}^{+}$ was observed, due to the presence of a reduced Ni center. The average $Ni–N_{eq}$ distance (2.024 Å) and Ni–Cl bond distance (2.361 Å) are significantly elongated (by ~0.160 Å), while the average $Ni–N_{ax}$ bond distance (2.193 Å) is only marginally increased (by 0.034 Å) *vs*. those in $\mathbf{1}^{+}$. Importantly, the addition of $PhICl_2$ into the solution of photo-generated $\mathbf{2}^{+}$ (irradiated solution of $\mathbf{1}^{+}$) led to an enhancement of the absorption band at 560 nm (Figure S8) and a color change to dark purple, which is in agreement with the regeneration of$\mathbf{1}^{+}$.

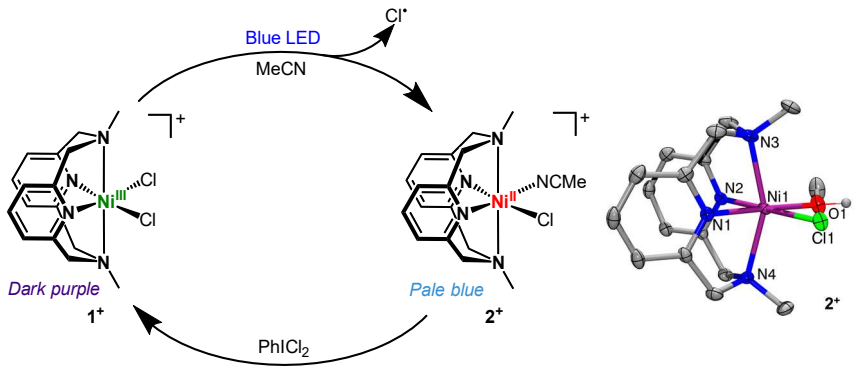


**Figure 4.** (left) Photolysis of $\mathbf{1}^{+}$ affording photoreduced $Ni^{II}$ complex $\mathbf{2}^{+}$ and regeneration of $\mathbf{1}^{+}$ achieved with $PhICl_2$. (right) ORTEP representation of $\mathbf{2}^{+}$. Ellipsoids are shown at 50% probability level, with carbon-bound hydrogen atoms, counterion and an outer-sphere solvent molecule eliminated for clarity. Selected bond lengths (Å): Ni1–N1 2.009(3), Ni–N2 2.034(3), Ni–N3 2.197(3), Ni–N4 2.189(3), Ni–Cl1 2.3611(8), Ni–O1 2.065(3).

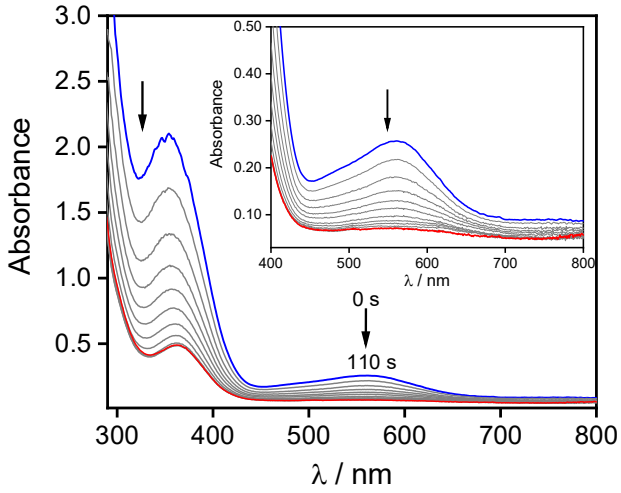


**Figure 5.** Photolysis of 1.3 mM MeCN solution of $\mathbf{1}^{+}$ with 456 nm blue LED excitation. The initial spectrum (blue line) converts to that of $\mathbf{2}^{+}$ (red line) over the course of 110 s. Spectra were recorded every 10 s.

Finally, the solid-state photoreduction of $\mathbf{1}^{+}$ into $\mathbf{2}^{+}$ was also tested. Irradiation of solid [**1**]$BF_4$ showed noticeable signs of discoloration from dark purple to light blue (Figure S9), indicating that halide photoelimination from a N-donor supported $Ni^{III}$ complex can also be promoted in the solid state. Additionally, photolysis of solid [**1**]$BF_4$ in THF was performed with a radical trapping agent, *N*-*tert*-butyl-α-phenylnitrone (PBN) (Figure S10). The EPR spectrum of the reaction mixture supports the formation of the PBN-THF adduct ($g$ = 2.0061, $A_N$ = 14.6 G, $A_H$ = 3.0 G, $A_C$(THF) = 3.0 G, $A_H$(THF) = 0.90 G), as the superhyperfine coupling constants of the spin adduct agreed well with reported values (Figure 6).[53,54] The PBN-THF spin adduct is believed to be formed through H atom abstraction by the photoeliminated chlorine radical and this is reminiscent of the work described by Castellano *et al.*, in which the PBN-THF spin adduct has been detected after Cu–Cl bond cleavage.[23]

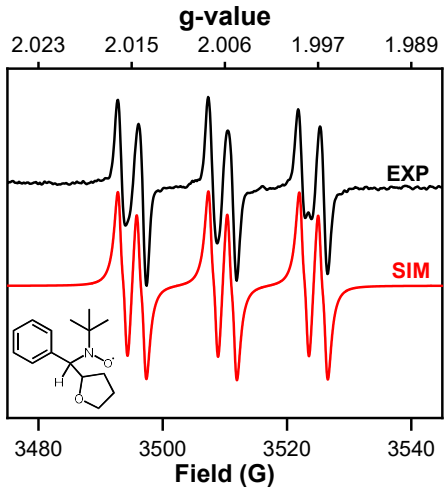


**Figure 6.** EPR spectrum of irradiated solid $\mathbf{1}^+$ in the presence of PBN. Parameters used for simulation: $g$ = 2.0061, $A_N$ = 14.6 G, $A_H$ = 3.0 G, $A_C$(THF) = 3.0 G, $A_H$(THF) = 0.90 G, linewidth 1.15 G.

## Conclusion

In conclusion, herein we are reporting a $Ni^{III}$ dichloride complex ($\mathbf{1}^+$) supported by a tetradentate N-donor pyridinophane ligand ($^{Me}$N4) and its photoinduced halogen elimination reactivity. The $^{Me}$N4 ligand can successfully stabilize a $Ni^{III}$ dichloride complex $\mathbf{1}^+$, allowing for isolation and detailed investigation of its photochemistry at RT. The titled complex was photoreduced upon blue light excitation, with elimination of chloride in the absence of a chemical trap. Characterization of the photoreduced Ni product and EPR spin trapping experiments provided evidence for the chlorine elimination reaction. TD-DFT calculations suggest that blue light excitation of $\mathbf{1}^+$ resulted in population of the LUMOs possessing Ni–Cl σ* character, corresponding to a photodissociative LMCT state. An important aspect of this work is the isolation, characterization, and photoreactivity study of a high-valent Ni dichloride complexes supported by a multidentate N-donor ligand, that appears to bear no precedent. This work may offer a platform not only for a photocatalytic HX splitting cycle, but also for related photoredox cross-coupling catalytic systems

involving photochemically generated radical species. Current studies are targeting on the examination of the photophysics and photochemistry of stable $[(^{R}N4)Ni^{III}ArX]^{+}$ (X = halide) complexes reported by our group,[28] which are also relevant to the commonly proposed photoactive Ni complexes in cross-coupling catalysis.

**Acknowledgement**

The authors acknowledge the National Science Foundation (CHE-1925751) for funding.

**TOC**

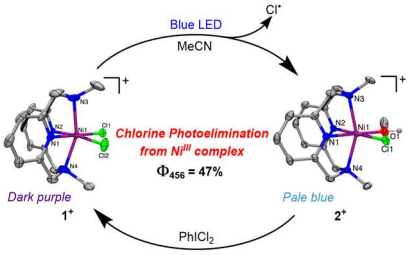


**References**

1 A. J. Esswein, D. G. Nocera, *Chem. Rev.*, 2007, **107**, 4022.

2 D. G. Nocera, *Inorg. Chem.*, 2009, **48**, 10001.

3 T. S. Teets, D. G. Nocera, *Chem. Comm.*, 2011, **47**, 9268.

4 L. Troian-Gautier, M. D. Turlington, S. A. M. Wehlin, A. B. Maurer, M. D. Brady, W. B. Swords, G. J. Meyer, *Chem. Rev.*, 2019, **119**, 4628.

5 T. R. Cook, A. J. Esswein, D. G. Nocera, *J. Am. Chem. Soc.*, 2007, **129**, 10094.

6 T. R. Cook, Y. Surendranath, D. G. Nocera, *J. Am. Chem. Soc.*, 2009, **131**, 28.

7 T. S. Teets, D. G. Nocera, *J. Am. Chem. Soc.*, 2009, **131**, 7411.

8 T. S. Teets, D. A. Lutterman, D. G. Nocera, *Inorg. Chem.*, 2010, **49**, 3035.

9 T. R. Cook, B. D. McCarthy, D. A. Lutterman, D. G. Nocera, *Inorg. Chem.*, 2012, **51**, 5152.

10 T.-P. Lin, F. P. Gabbai, *J. Am. Chem. Soc.*, 2012, **134**, 12230.

11 H. Yang, F. P. Gabbaï, *J. Am. Chem. Soc.*, 2014, **136**, 10866.

12 T. A. Perera, M. Masjedi, P. R. Sharp, *Inorg. Chem.*, 2014, **53**, 7608.

13 D. C. Powers, M. B. Chambers, T. S. Teets, N. Elgrishi, B. L. Anderson, D. G. Nocera, *Chem. Sci.*, 2013, **4**, 2880.

14 R. M. Izatt, S. R. Izatt, R. L. Bruening, N. E. Izatt, B. A. Moyer, *Chem. Soc. Rev.*, 2014, **43**, 2451.

15 C. Förster, K. Heinze, *Chem. Soc. Rev.*, 2020, **49**, 1057.

16 S. J. Hwang, B. L. Anderson, D. C. Powers, A. G. Maher, R. G. Hadt, D. G. Nocera, *Organometallics*, 2015, **34**, 4766.

17 S. J. Hwang, D. C. Powers, A. G. Maher, B. L. Anderson, R. G. Hadt, S.-L. Zheng, Y.-S. Chen, D. G. Nocera, *J. Am. Chem. Soc.*, 2015, **137**, 6472.

18 P. T. Matsunaga, G. L. Hillhouse, A. L. Rheingold, *J. Am. Chem. Soc.*, 1993, **115**, 2075.

19 R. Y. Han, G. L. Hillhouse, *J. Am. Chem. Soc.*, 1997, **119**, 8135.

20 K. Koo, G. L. Hillhouse, *Organometallics*, 1995, **14**, 4421.

21 K. M. Koo, G. L. Hillhouse, A. L. Rheingold, *Organometallics*, 1995, **14**, 456.

22 D. C. Powers, B. L. Anderson, D. G. Nocera, *J. Am. Chem. Soc.*, 2013, **135**, 18876.

23 R. Fayad, S. Engl, E. O. Danilov, C. E. Hauke, O. Reiser, F. N. Castellano, *The Journal of Physical Chemistry Letters*, 2020, **11**, 5345.

24 B. J. Shields, A. G. Doyle, *J. Am. Chem. Soc.*, 2016, **138**, 12719.

25 L. K. G. Ackerman, J. I. Martinez Alvarado, A. G. Doyle, *J. Am. Chem. Soc.*, 2018, **140**, 14059.

26 S. K. Kariofillis, A. G. Doyle, *Acc. Chem. Res.*, 2021, **54**, 988.

27 D. R. Heitz, J. C. Tellis, G. A. Molander, *J. Am. Chem. Soc.*, 2016, **138**, 12715.

28 B. Zheng, F. Z. Tang, J. Luo, J. W. Schultz, N. P. Rath, L. M. Mirica, *J. Am. Chem. Soc.*, 2014, **136**, 6499.

29 F. Z. Tang, N. P. Rath, L. M. Mirica, *Chem. Comm.*, 2015, **51**, 3113.

30 W. Zhou, S. A. Zheng, J. W. Schultz, N. P. Rath, L. M. Mirica, *J. Am. Chem. Soc.*, 2016, **138**, 5777.

31 J. W. Schultz, K. Fuchigami, B. Zheng, N. P. Rath, L. M. Mirica, *J. Am. Chem. Soc.*, 2016, **138**, 12928.

32 M. B. Watson, N. P. Rath, L. M. Mirica, *J. Am. Chem. Soc.*, 2017, **139**, 35.

33 P. Mondal, P. Pirovano, A. Das, E. R. Farquhar, A. R. McDonald, *J. Am. Chem. Soc.*, 2018, **140**, 1834.

34 J. B. Diccianni, C. H. Hu, T. N. Diao, *Angew. Chem., Int. Ed.*, 2016, **55**, 7534.

35 R.-J. Cheng, C.-H. Ting, T.-C. Chao, T.-H. Tseng, P. P. Y. Chen, *Chem. Comm.*, 2014, **50**, 14265.

36 N. Kuwamura, K. i. Kitano, M. Hirotsu, T. Nishioka, Y. Teki, R. Santo, A. Ichimura, H. Hashimoto, L. J. Wright, I. Kinoshita, *Chem. Eur. J.*, 2011, **17**, 10708.

37 K. A. Kozhanov, M. P. Bubnov, V. K. Cherkasov, G. K. Fukin, N. N. Vavilina, L. Y. Efremova, G. A. Abakumov, *J. Mag. Res.*, 2009, **197**, 36.

38 W. Zhou, N. P. Rath, L. M. Mirica, *Dalton Trans.*, 2016, **45**, 8693.

39 D. M. Grove, G. van Koten, R. Zoet, N. W. Murrall, A. J. Welch, *J. Am. Chem. Soc.*, 1983, **105**, 1379.

40 D. M. Grove, G. van Koten, P. Mul, R. Zoet, J. G. M. van der Linden, J. Legters, J. E. J. Schmitz, N. W. Murrall, A. J. Welch, *Inorg. Chem.*, 1988, **27**, 2466.

41 A. W. Kleij, R. A. Gossage, R. J. M. Klein Gebbink, N. Brinkmann, E. J. Reijerse, U. Kragl, M. Lutz, A. L. Spek, G. van Koten, *J. Am. Chem. Soc.*, 2000, **122**, 12112.

42 B. Mougang-Soumé, F. Belanger-Gariépy, D. Zargarian, *Organometallics*, 2014, **33**, 5990.

43 J.-P. Cloutier, D. Zargarian, *Organometallics*, 2018, **37**, 1446.

44 J. R. Khusnutdinova, J. Luo, N. P. Rath, L. M. Mirica, *Inorg. Chem.*, 2013, **52**, 3920.

45 D. F. Evans, *J. Chem. Soc.*, 1959, 2003.

46 J. Loliger, R. Scheffold, *J. Chem. Educ.*, 1972, **49**, 646.

47 D. M. Grove, G. Van Koten, P. Mul, A. A. H. Van der Zeijden, J. Terheijden, M. C. Zoutberg, C. H. Stam, *Organometallics*, 1986, **5**, 322.

48 D. M. Grove, G. Van Koten, P. Mul, R. Zoet, J. G. M. Van der Linden, J. Legters, J. E. J. Schmitz, N. W. Murrall, A. J. Welch, *Inorg. Chem.*, 1988, **27**, 2466.

49 L. A. van de Kuil, Y. S. J. Veldhuizen, D. M. Grove, J. W. Zwikker, L. W. Jenneskens, W. Drenth, W. J. J. Smeets, A. L. Spek, G. van Koten, *J. Organomet. Chem.*, 1995, **488**, 191.

50 V. M. Iluc, A. J. M. Miller, J. S. Anderson, M. J. Monreal, M. P. Mehn, G. L. Hillhouse, *J. Am. Chem. Soc.*, 2011, **133**, 13055.

51 see ESI for details.

52 R. L. Martin, *J. Chem. Phys.*, 2003, **118**, 4775.

53 Y. Kotake, K. Kuwata, *Bull. Chem. Soc. Jpn.*, 1981, **54**, 394.

54 G. R. Buettner, *Free Radic. Biol. Med.*, 1987, **3**, 259.